

Supplementary material for LHCb-PAPER-2016-063

Figures 5, 6, 7, 8 and 9 are from the analysis based on Eq. (1) and Figs. 10, 11, 12, 13, 14 and 15 from the analysis based on Eq. (2).

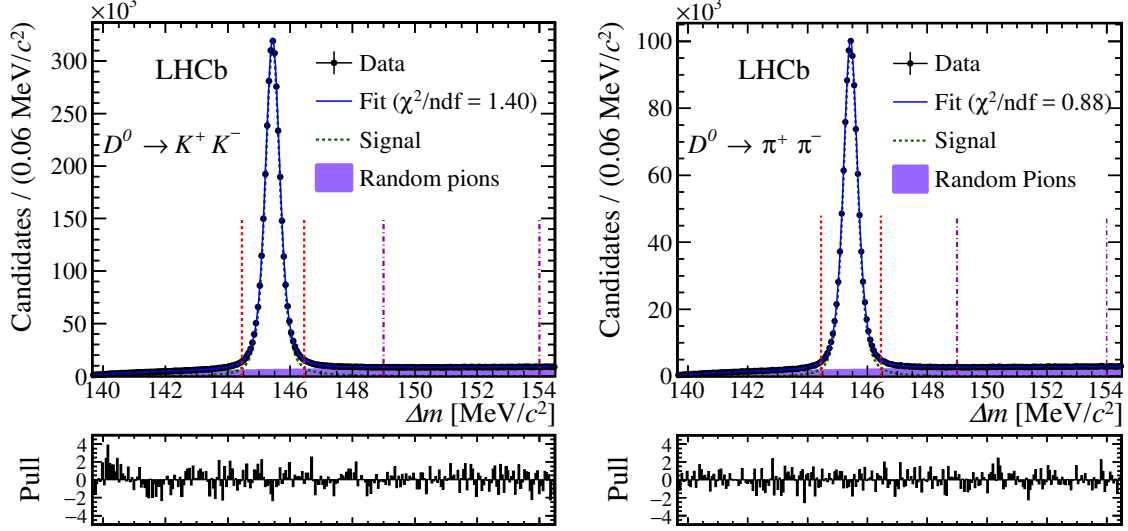


Figure 5: Distribution of the invariant mass difference $\Delta m \equiv m(D^0 \pi^+) - m(D^0)$, in the 2012 *MagDown* subsample for the (left) $D^0 \rightarrow K^+ K^-$ and (right) $D^0 \rightarrow \pi^+ \pi^-$ candidates, with results of the fits included. Black dots are data points, while the solid blue line is the total fit projection. The signal component is represented by the dashed green line, while the random pion background is represented by the filled purple area. Dashed red and dash-dotted purple lines indicate signal and sideband regions respectively. A Johnson S_U -distribution plus the sum of three Gaussian functions is used to model the signal, while the background is described by an empirical function of the form $1 - \exp[(\Delta m - \Delta m_0)/\alpha] + \beta(\Delta m/\Delta m_0 - 1)$, where Δm_0 is the threshold of the function, and α and β describe its shape. The residuals between data and the fit are shown in units of the statistical standard deviation, labelled as pull.

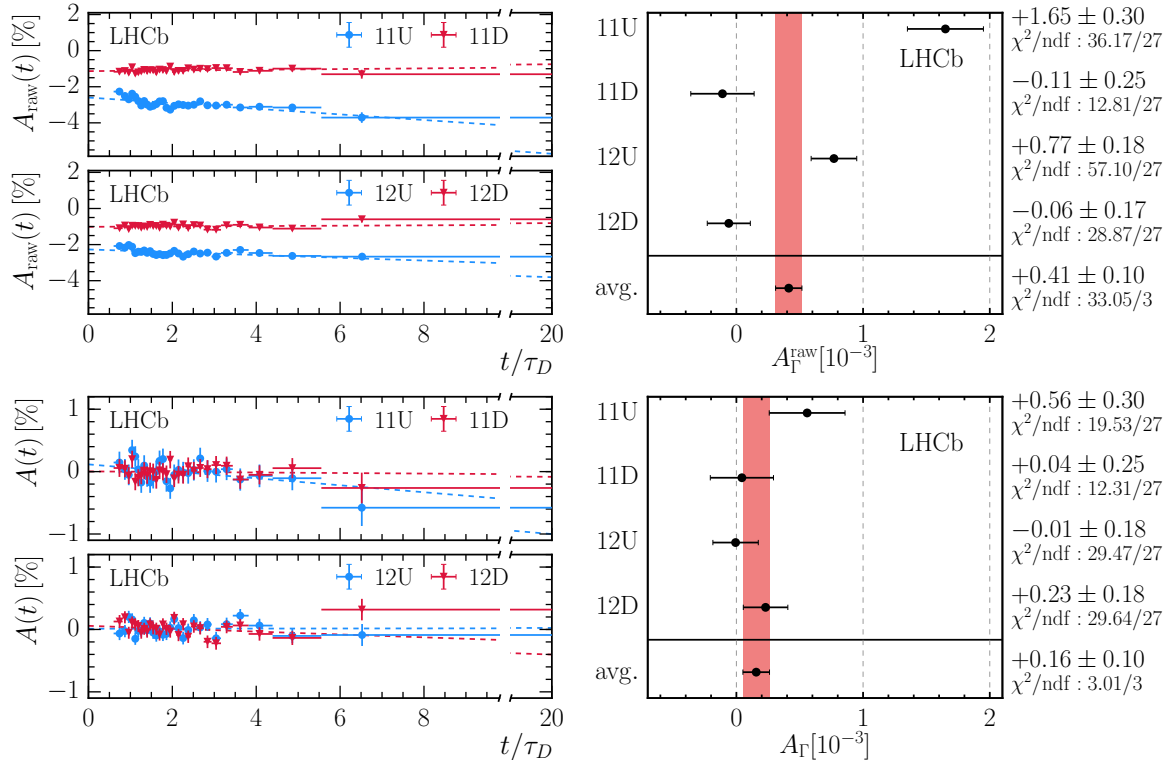


Figure 6: Measured (top left) raw asymmetry and (bottom left) corrected asymmetry in bins of t/τ_D , where $\tau_D = 0.410$ ps [16], for the $D^0 \rightarrow K^- \pi^+$ decay mode. The results obtained in the four subsamples are shown, with fit results included (dashed lines). Results for $A_{\Gamma}(D^0 \rightarrow K^- \pi^+)$ (top) before and (bottom) after the correction are reported on the right, where the label 2011 (2012) is abbreviated 11 (12) and *MagUp* (*MagDown*) is abbreviated U(D). The weighted average (avg.) of the four A_{Γ} values is indicated by the colored vertical band.

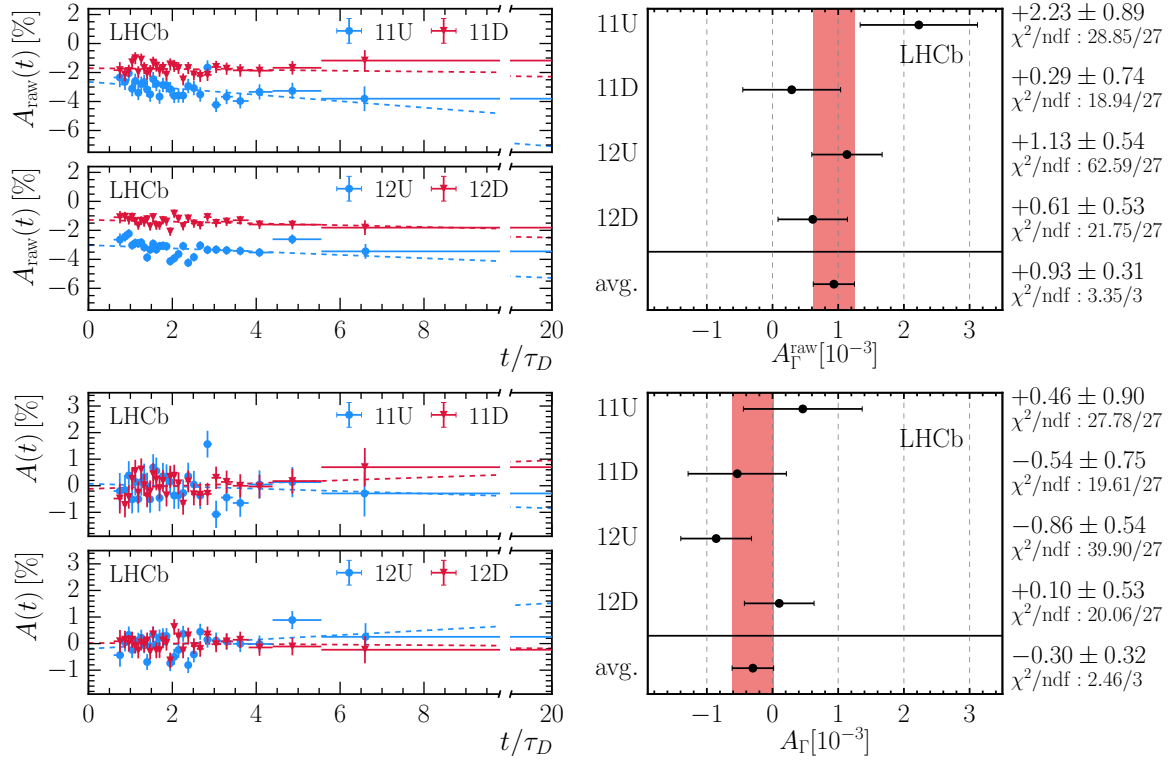


Figure 7: Measured (top left) raw asymmetry and (bottom left) corrected asymmetry in bins of t/τ_D , where $\tau_D = 0.410$ ps [16], for the $D^0 \rightarrow K^+ K^-$ decay mode. The results obtained in the four subsamples are shown, with fit results included (dashed lines). Results for $A_\Gamma(D^0 \rightarrow K^+ K^-)$ (top) before and (bottom) after the correction are reported on the right, where the label 2011 (2012) is abbreviated 11 (12) and *MagUp* (*MagDown*) is abbreviated U(D). The weighted average (avg.) of the four A_Γ values is indicated by the colored vertical band.

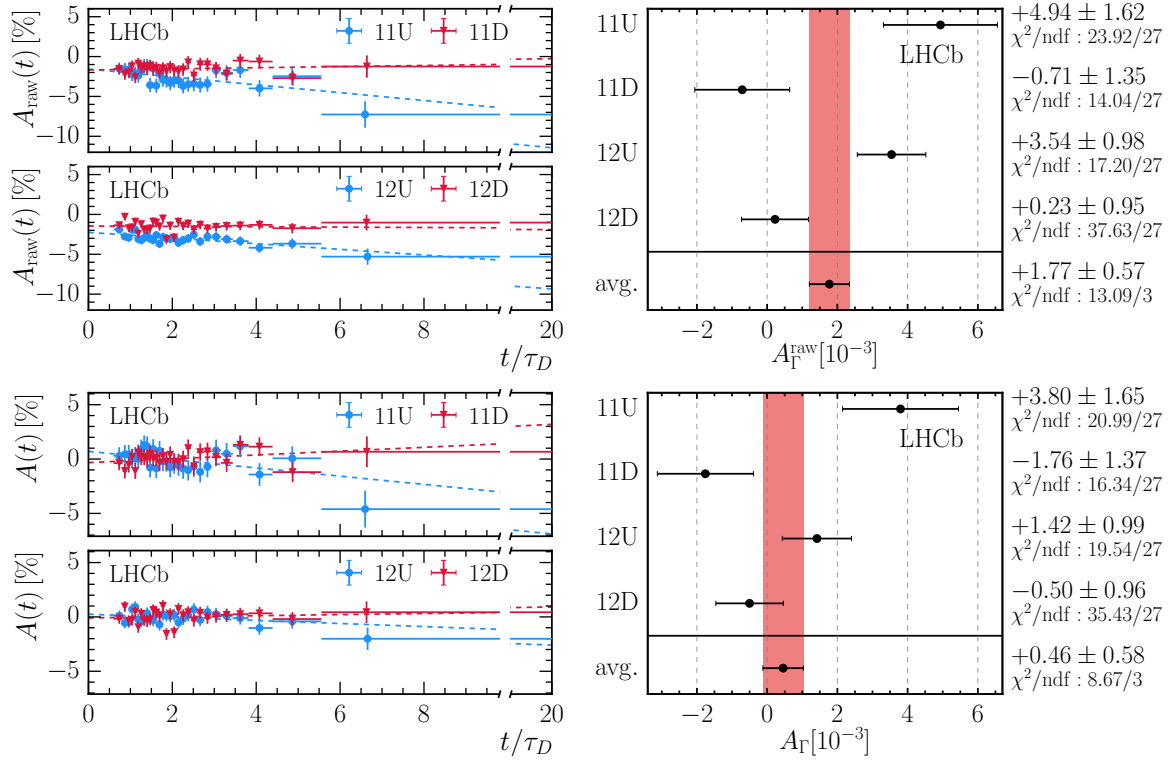


Figure 8: Measured (top left) raw asymmetry and (bottom left) corrected asymmetry in bins of t/τ_D , where $\tau_D = 0.410$ ps [16], for the $D^0 \rightarrow \pi^+\pi^-$ decay mode. The results obtained in the four subsamples are shown, with fit results included (dashed lines). Results for $A_\Gamma(D^0 \rightarrow \pi^+\pi^-)$ (top) before and (bottom) after the correction are reported on the right, where the label 2011 (2012) is abbreviated 11 (12) and *MagUp* (*MagDown*) is abbreviated U(D). The weighted average (avg.) of the four A_Γ values is indicated by the colored vertical band.

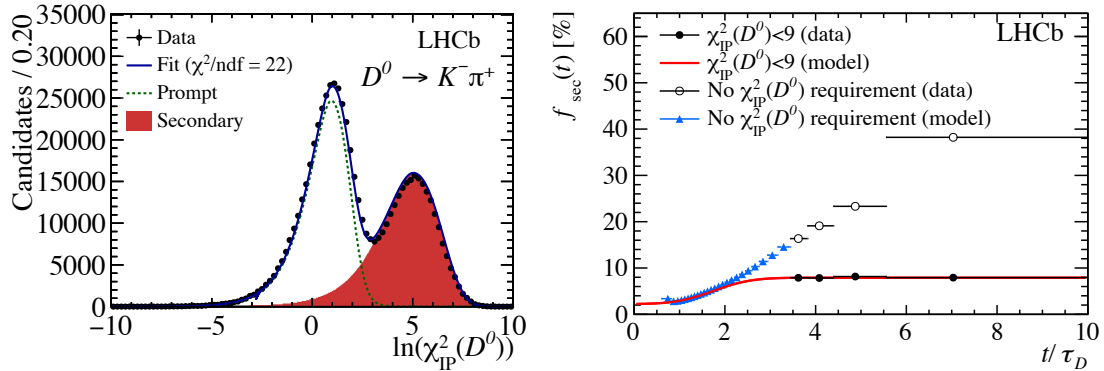


Figure 9: Distribution (left) of $\ln(\chi_{\text{IP}}^2(D^0))$ with $t/\tau_D \in [5.55, 20]$ in the 2012 *MagDown* subsample, with fit results overlaid, and (right) fraction of secondary decays $f_{\text{sec}}(t)$ as a function of t/τ_D . These plots illustrate the method used to estimate the relative fraction of secondary charm decays $f_{\text{sec}}(t)$. For large decay times ($t/\tau_D > 3.4$), where the secondary component is sizable and well distinguishable from the prompt component, a fit of the distribution of $\chi_{\text{IP}}^2(D^0)$ in each bin allows the estimation of $f_{\text{sec}}(t)$ from data, both with and without the $\chi_{\text{IP}}^2(D^0) < 9$ requirement. An example of these fits is reported on the left, corresponding to the higher time bin. The values of $f_{\text{sec}}(t)$ without $\chi_{\text{IP}}^2(D^0)$ requirement are used to constrain the normalization of an acceptance-corrected analytical model of the number of secondary decays, given by the convolution of two exponentials having as slopes the average lifetime of a mixture of b hadrons ($\tau_b = 1.568$ ps [16]) and the average lifetime of the D^0 meson ($\tau_D = 0.410$ ps [16]). The value of $f_{\text{sec}}(t)$ in the final sample with all requirements is then obtained by interpolation of the low-decay-time part of the model, that is unaffected by requirements, and the points at large decay times measured from data as explained above.

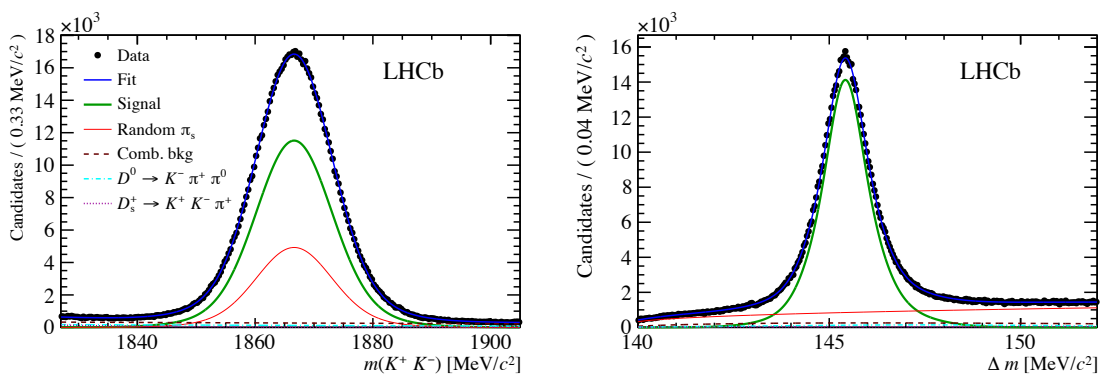


Figure 10: Distributions of (left) $m(K^+K^-)$ and (right) Δm for the the selected $D^* \rightarrow D^0\pi^+$, $D^0 \rightarrow K^+K^-$ candidates in the second of the three 2012 data taking periods and with magnetic field pointing downwards. The unbinned maximum likelihood fit results are overlaid.

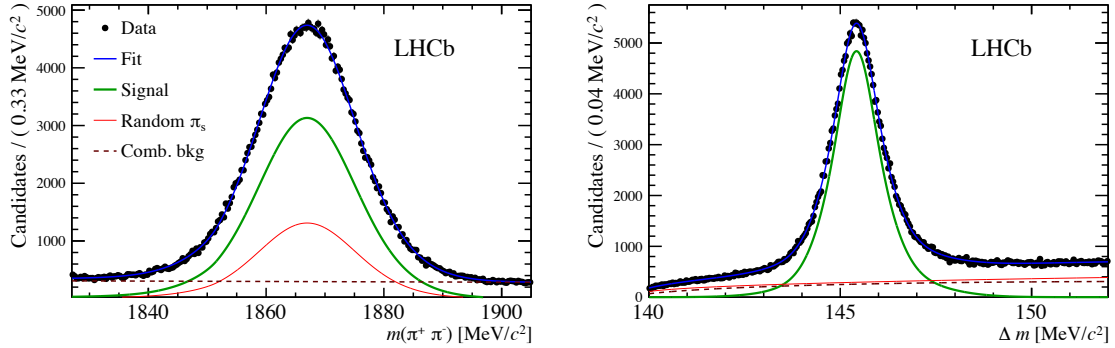


Figure 11: Distributions of (left) $m(\pi^+\pi^-)$ and (right) Δm for the the selected $D^* \rightarrow D^0\pi^+$, $D^0 \rightarrow \pi^+\pi^-$ candidates in the second of the three 2012 data taking periods and with magnetic field pointing downwards. The unbinned maximum likelihood fit results are overlaid.

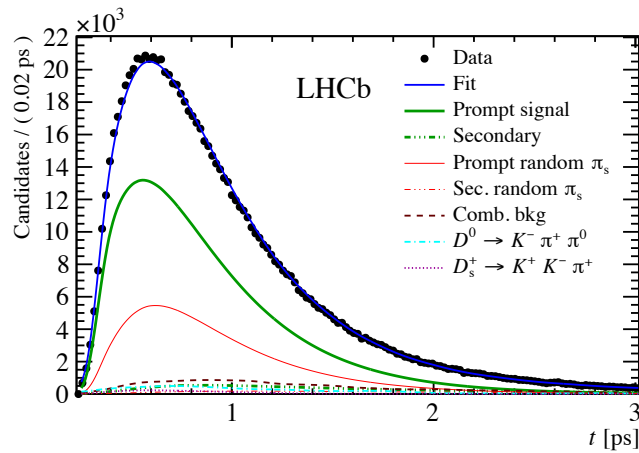


Figure 12: Distribution of decay time for the selected $D^0 \rightarrow K^+K^-$ candidates in the second of the three 2012 data taking periods with magnetic field pointing downwards. The unbinned maximum likelihood fit results are overlaid.

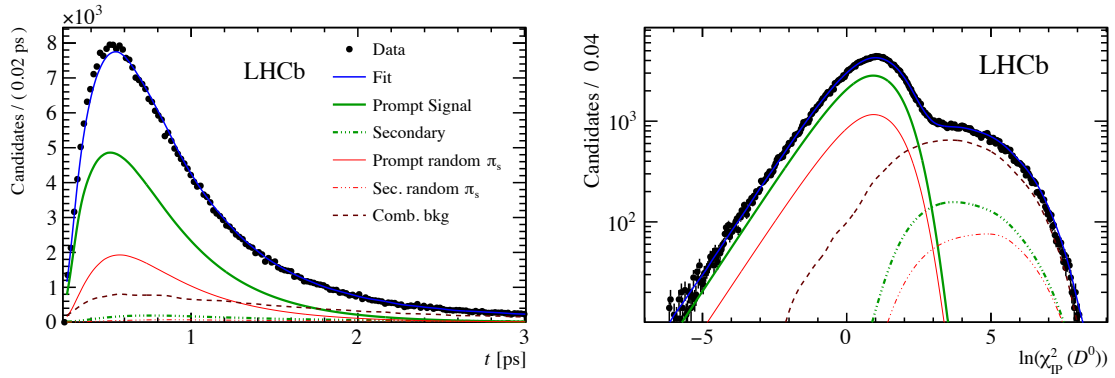


Figure 13: Distributions of (left) decay time and (right) $\ln(\chi_{\text{IP}}^2(D^0))$ for the selected $D^0 \rightarrow \pi^+\pi^-$ candidates in the second of the three 2012 data taking periods with magnetic field pointing downwards. The unbinned maximum likelihood fit results are overlaid. Gaussian kernels are used to smooth the combinatorial backgrounds.

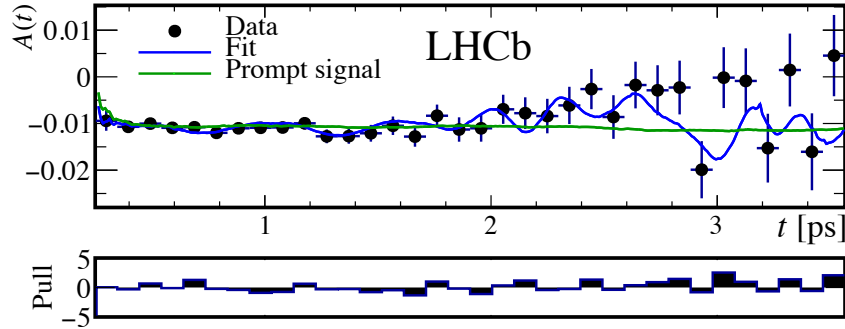


Figure 14: Asymmetry between D^0 and \bar{D}^0 data overlaid by the total unbinned maximum likelihood fit and prompt signal fit component for the K^+K^- final state. The data are from all 2012 subsets and the fit components are constructed from the individual fits to each subset. The residuals between data and fit are shown in units of the statistical standard deviation, labelled as pull.

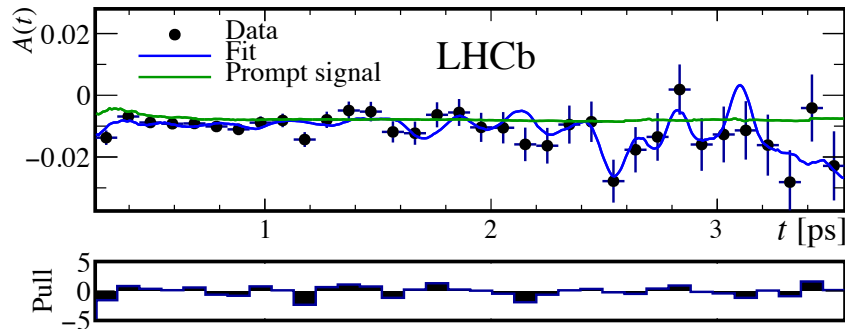


Figure 15: Asymmetry between D^0 and \bar{D}^0 data overlaid by the total unbinned maximum likelihood fit and prompt signal fit component for the $\pi^+\pi^-$ final state. The data are from all 2012 subsets and the fit components are constructed from the individual fits to each subset. The residuals between data and fit are shown in units of the statistical standard deviation, labelled as pull.